7-2017

Nonmeteorological Influences on Severe Thunderstorm Warning Issuance: A Geographically Weighted Regression-Based Analysis of County Warning Area Boundaries, Land Cover, and Demographic Variables

Megan L. White
University of Kentucky, megan.white1@uky.edu

J. Anthony Stallins
University of Kentucky, ja.stallins@uky.edu

Nonmeteorological Influences on Severe Thunderstorm Warning Issuance: A Geographically Weighted Regression-Based Analysis of County Warning Area Boundaries, Land Cover, and Demographic Variables

Notes/Citation Information
Published in *Weather, Climate, and Society*, v. 9, no. 3, p. 421-439.

Digital Object Identifier (DOI)
https://doi.org/10.1175/WCAS-D-15-0070.1

Nonmeteorological Influences on Severe Thunderstorm Warning Issuance: A Geographically Weighted Regression-Based Analysis of County Warning Area Boundaries, Land Cover, and Demographic Variables

MEGAN L. WHITE AND J. ANTHONY STALLINS

University of Kentucky, Lexington, Kentucky

(Manuscript received 25 November 2015, in final form 7 March 2017)

ABSTRACT

Studies have shown that the spatial distribution of severe thunderstorm warnings demonstrates variation beyond what can be attributed to weather and climate alone. Investigating spatial patterns of these variations can provide insight into nonmeteorological factors that might lead forecasters to issue warnings. Geographically weighted regression was performed on a set of demographic and land cover descriptors to ascertain their relationships with National Weather Service (NWS) severe thunderstorm warning polygons issued by 36 NWS forecast offices in the central and southeastern United States from 2008 to 2015. County warning area (CWA) boundaries and cities were predominant sources of variability in warning counts. Global explained variance in verified and unverified severe thunderstorm warnings ranged from 67% to 81% for population, median income, and percent imperviousness across the study area, which supports the spatial influence of these variables on warning issuance. Local regression coefficients indicated that verified and unverified warning counts increased disproportionately in larger cities relative to the global trend, particularly for NWS weather forecast office locations. However, local explained variance tended to be lower in cities, possibly due to greater complexity of social and economic factors shaping warning issuance. Impacts of thunderstorm type and anthropogenic modification of existing storms should also be considered when interpreting the results of this study.

1. Introduction

Severe thunderstorm warnings (SVTs) are issued by the National Weather Service (NWS) when convective outbreaks are capable of producing hail with a diameter of 1 in. or greater, and/or winds at speeds of 58 mph or greater. Accurate warnings are essential for alerting affected areas that human and property risk are elevated, and that appropriate precautions should be taken. Meteorologists at local Weather Forecast Offices (WFOs) of the NWS rely on Doppler radar and computer algorithms to delineate regions of severe thunderstorm risk in their respective county warning areas (CWAs). Visual observations and data reported by trained storm spotters, the general public, and weather station personnel may be used as supplemental information to determine whether a severe warning is necessary.

Although institutional standards structure the warning process, human factors also influence the issuance of SVTs. The density of spotters is often sparse in rural areas, so events may go unwarned. Social and behavioral factors shape the warning process as well (Sander et al. 2013; Allen et al. 2016). For example, knowledge of the underlying distribution of population across a forecast area may make a forecaster more or less likely to release a warning (Davis and LaDue 2004; Barrett 2008). This sensitivity can be associated not only with forecaster awareness of greater potential for damage but also with the reality that larger numbers of people imply greater likelihood of severe weather phenomena being spotted, reported, and employed to issue or verify a warning. Forecasters may then become conditioned to warn one area over another based on their perception of how likely it is that a field observation will confirm severe status. In addition, high population areas may report greater numbers of warnings for marginally severe storms than less populated areas. Consequently, forecasters may overlook borderline severe storms where they would be less likely to be reported in the first place (Dobur 2005). Alongside sensitivities to population increases, an area's economic status has been shown to correspond with forecasting outcomes as well. Anbarci et al. (2011) found "economic sensitivity" in weather

Corresponding author: Megan L. White, megan.white1@uky.edu

DOI: 10.1175/WCAS-D-15-0070.1

forecasting, in which NWS forecast accuracy improved with increases in income. In an earlier paper, Anbarci et al. (2008) noted that both the NWS and private weather forecasting companies produce forecasts of significantly higher accuracy for areas with greater market extent, which for these purposes can be defined as areas having more people and more economic resources.

In general, criteria for establishing damage reports tend to favor urban criteria versus rural (Guyer and Moritz 2003). As a phenomenon of severe thunderstorms, tornado warnings can be skewed toward more populated areas, where they are more readily verified on the ground (Brooks et al. 2003; Frisbie 2006). Elsner et al. (2013) suggested that the weakening population bias in tornado reports in the central plains of the United States between 2002 and 2011 is attributable to an increase in storm chaser presence in rural areas. Other influences include the expanding bull's-eye of population and built environment (Ashley et al. 2014; Rosencrants and Ashley 2015). An increase over time in severe weather reports can be partly attributed to a greater human population density (Ray et al. 2003; Paulikas 2013).

There are only a few systematic multicity examinations of how the underlying population relates to severe thunderstorm warnings. In the Atlanta metropolitan region in Georgia (Dobur 2005), severe thunderstorm warnings were more numerous in counties designated as urban as opposed to rural. However, for the forecast areas around Raleigh, North Carolina, neither population density nor per capita income were associated with counts of severe thunderstorm warnings (Hoium et al. 1997). Barrett (2008) used linear regression to examine relationships in central Texas between SVTs, population, and distance from the WFO. Although the results were weakly significant, there was evidence for a population bias for the entire study area, and within almost all of the individual CWAs. In a later study (Barrett 2012), the patterns of SVTs over a 14-yr period (1996–2010) had a strong statistical relationship with population, although this could vary according to whether the warnings were issued for individual storms or at a level that encompassed an entire county. Barrett also discusses how some CWAs received awards for excellence in severe weather-related service, while others were given more punitive recognition for undesired forecast practices, and relates these considerations to the outcomes of his study.

The location of forecast offices and radar sites is also relevant for assessing the human influence on warning issuance and verification. WFOs and radar sites frequently are situated just west or southwest of densely populated areas (Fine 2007, p. 24). This arrangement enhances the likelihood that radar will detect severe weather before it reaches the populated area due to prevailing westerly winds. These locations are also filled with trained staff watching for signs of severe thunderstorms, using equipment whose specialized purpose is to detect the weather system. At the very least, these factors make the more populated areas and the WFO locations high confidence points in terms of accurate and verified reports (Ray et al. 2003; Doswell et al. 2005).

WFOs are urged by the NWS to reduce the number of false alarms they issue for severe weather to avoid a high false alarm ratio (FAR; Barnes et al. 2007). A warning is considered a false alarm when wind speed and hail size criteria are either unmet or unverified following the issuance of the warning. The FAR for a WFO is equal to the fraction of false or unverified warnings to the total number of warnings issued. Conventional wisdom holds that repeatedly issuing false alarms is potentially dangerous because of the desensitization it may engender within the warned population (Barnes et al. 2007). Overissuing warnings has also been shown to have negative economic impacts on affected areas (Sutter and Erikson 2010), which puts additional pressure on WFOs to produce accurate forecasts and warnings. Given these operational factors, the influence of the recent track record of verified-versus-unverified warnings at a WFO may be reflected in an office's tendency to issue or not issue a severe weather warning. This illustrates how, to some degree, information collection practices and their communication can differ from one WFO to the next and make the decision to issue a warning a more contextual event (Hales 1993; Lindell and Brooks 2013).

An array of institutional and behavioral factors influences how forecasters, spotters, and the general public respond to severe weather events and warnings (Morss and Ralph 2007; Pennell 2009; Schmidlin et al. 2009; Lindell and Brooks 2013). Systematic analysis of all of them and identification of their causal importance are beyond the scope of this study. However, the potential influence of local WFO culture and forecaster practices on SVTs can be explored through an examination of their spatial association. Geographically weighted regression (GWR) was employed in this study to illuminate how local warning issuance varies in relation to WFO jurisdictions and to three indicators of human presence: population, income, and percent impervious cover. Population and income as potential drivers of warning issuance were addressed directly in the preceding paragraphs; we feel that percent impervious cover is relevant in this analysis because of its association with development and market extent (see Anbarci et al. 2008). GWR facilitated discrimination between locations that are overwarned and locations that are underwarned in relation to the general warning trends across a broad area with a heterogeneous arrangement of urban and rural

locales. While GWR was used to quantify local deviations in the relationships between warnings and these three independent variables, we did not definitively attribute these deviations as inherently related to human decision-making processes or to meteorological conditions. GWR allows us to visualize statistical associations and to begin hypothesizing about how human factors and meteorological conditions influence warning records, including the potential for their interaction in the form of anthropogenic modification of convective processes (Rozoff et al. 2003; Gero and Pitman 2006; Haberlie et al. 2015).

2. Methods

We posed two questions: 1) How do population, income, and percent impervious surface vary in their association with the number of verified and unverified severe thunderstorm warnings? 2) What role do CWA boundaries and WFO locations play in the response patterns of verified and unverified warnings to the independent variables? The geographic extent of our study spanned 13 states of the central and southeastern United States in their entirety, and portions of 7 additional states. The study area spans several National Climatic Data Center regions (NOAA 2016) and three NWS regions. This particular area of study was chosen to achieve a balance between climatic consistency and the ability to identify contrasts among forecasting cultures, should they be present. It also spans a latitudinal gradient in type and frequency of thunderstorms. In general, the number of supercell thunderstorms is higher in the more central inland regions of the study area, while sea-breeze and maritime convective processes limit large, severe thunderstorm development in coastal areas.

a. Data

1) SEVERE THUNDERSTORM WARNING POLYGONS

ArcGIS shapefiles for NWS severe weather warning polygons were obtained from an archive maintained by Iowa State University's Iowa Environmental Mesonet (IEM 2016). These polygons show the bounded areas of all severe thunderstorm warnings issued by the NWS for the United States. The polygons include initial warning polygons, as well as subsequent polygons representing the movement and modifications of these initial polygons through warning expiration. Some of these warning polygons are storm based and delineate irregular storm boundaries. Others are countywide warnings and follow the outlines of individual counties. Multiple severe thunderstorm warning polygons can be issued for a single thunderstorm event, some of which will overlap.

Verification status is included in the IEM data, but in some cases it is still preliminary.

Before being recorded into NWS Storm Data, the more authoritative source of verified events, the validity and accuracy of warnings are checked, and sometimes updated. Official verification records from NWS Storm Data were used to designate each SVT polygon as verified versus unverified. Initially, a total of 266 887 severe thunderstorm warnings occurred over the 8-yr duration of our data. However, discrepancies between IEM data and NWS Storm Data resulted in 1036 polygons with no verification status. These 1036 polygons were approximately 0.4% of the total and are not included in the analysis. Inspection of the polygons indicated that they were randomly distributed among WFOs and were sometimes issued as part of the same thunderstorm event. Of the remaining 265 851 warnings, 160 544 were verified and 105 307 were unverified. We analyzed counts as verified and unverified rather than combining them into a FAR because FAR is a relativized value. Its use would eliminate variations related to the raw number of thunderstorm warnings. The actual number of thunderstorms experienced by an area may be important to how forecasters are conditioned to issue warnings. For example, rather than equate St. Louis, Missouri, with south Florida because they have the same FAR, we compared verified and unverified counts directly.

2) INDEPENDENT VARIABLES

The 2006 National Land Cover Dataset is derived from imagery captured by the Enhanced Thematic Mapper Plus (ETM+) sensor on board *Landsat 7*. These data are produced at a 30-m spatial resolution (Fry et al. 2011). Synchronous with the development of the NLCD, a percent imperviousness dataset was produced at the same scale from the same imagery. Total population and median income at the level of census tracts were obtained from the American Community Survey via the U.S. Census Bureau's American FactFinder. The American Community Survey (ACS) is an ongoing national survey distributed to randomly selected households and is used to produce period estimates of numerous demographic variables (U.S. Census Bureau 2013). ACS 5-yr estimates in this study are for the years 2007–11.

b. Database assembly

All preprocessing and data assembly were performed in ArcGIS, version 10.1, and integrated into a USA Contiguous Lambert conformal conic projection. The geographic extent of the 36 CWAs (Table 1; Fig. 1) was used to clip SVT polygons and data for percent impervious cover, total population, and median income. All data were joined to a rectangular grid of 20 × 20 km

TABLE 1. WFO cities and regions in this study.

Office Code	Forecast Office
AKQ	Wakefield, VA
BMX	Birmingham, AL
CAE	Columbia, SC
CHS	Charleston, SC
CLE	Cleveland, OH
DVN	Davenport/Quad Cities, IA
FFC	Peachtree City–Atlanta, GA
GSP	Greenville–Spartanburg, SC
HUN	Huntsville, AL
ILM	Wilmington, NC
ILN	Wilmington, OH
ILX	Lincoln, IL
IND	Indianapolis, IN
IWX	Northern Indiana
JAN	Jackson, MS
JAX	Jacksonville, FL
JKL	Jackson, KY
LIX	New Orleans–Baton Rouge, LA
LMK	Louisville, KY
LOT	Chicago, IL
LSX	St. Louis, MO
LWX	Baltimore, MD–Washington, D.C.
MEG	Memphis, TN
MFL	Miami, FL
MHX	Newport–Morehead City, NC
MLB	Melbourne, FL
MOB	Mobile, AL–Pensacola, FL
MRX	Morristown–Knoxville, TN
OHX	Nashville, TN
PAH	Paducah, KY
PBZ	Pittsburgh, PA
RAH	Raleigh, NC
RLX	Charleston, WV
RNK	Blacksburg, VA
TAE	Tallahassee, FL
TBW	Tampa, FL

cells. Based on pilot analyses, 10- and 50-km grid sizes were not optimal for interpreting SVT patterns in relation to the size of cities and CWA boundaries.

The total population for an individual grid cell was derived from the sum of population values for each census tract centroid falling within a cell. An estimate of income within each grid cell was determined by taking the average of the centroids for each of the tracts that fell within a grid cell. Block statistics were employed in ArcGIS to convert the NLCD impervious data to 20 km × 20 km resolution. Regional and urban–rural contrasts were evident in each of these three independent variables (Fig. 2). Pearson's correlation coefficients for the gridcell values of each independent variable indicated a high positive correlation of population and impervious cover ($r = 0.92$, $p < 0.001$), followed by impervious cover and median income ($r = 0.26$, $p < 0.001$) and population and median income ($r = 0.27$, $p < 0.001$).

FIG. 1. (top) WFO cities and their forecast zone boundaries; (bottom) other larger cities in study area.

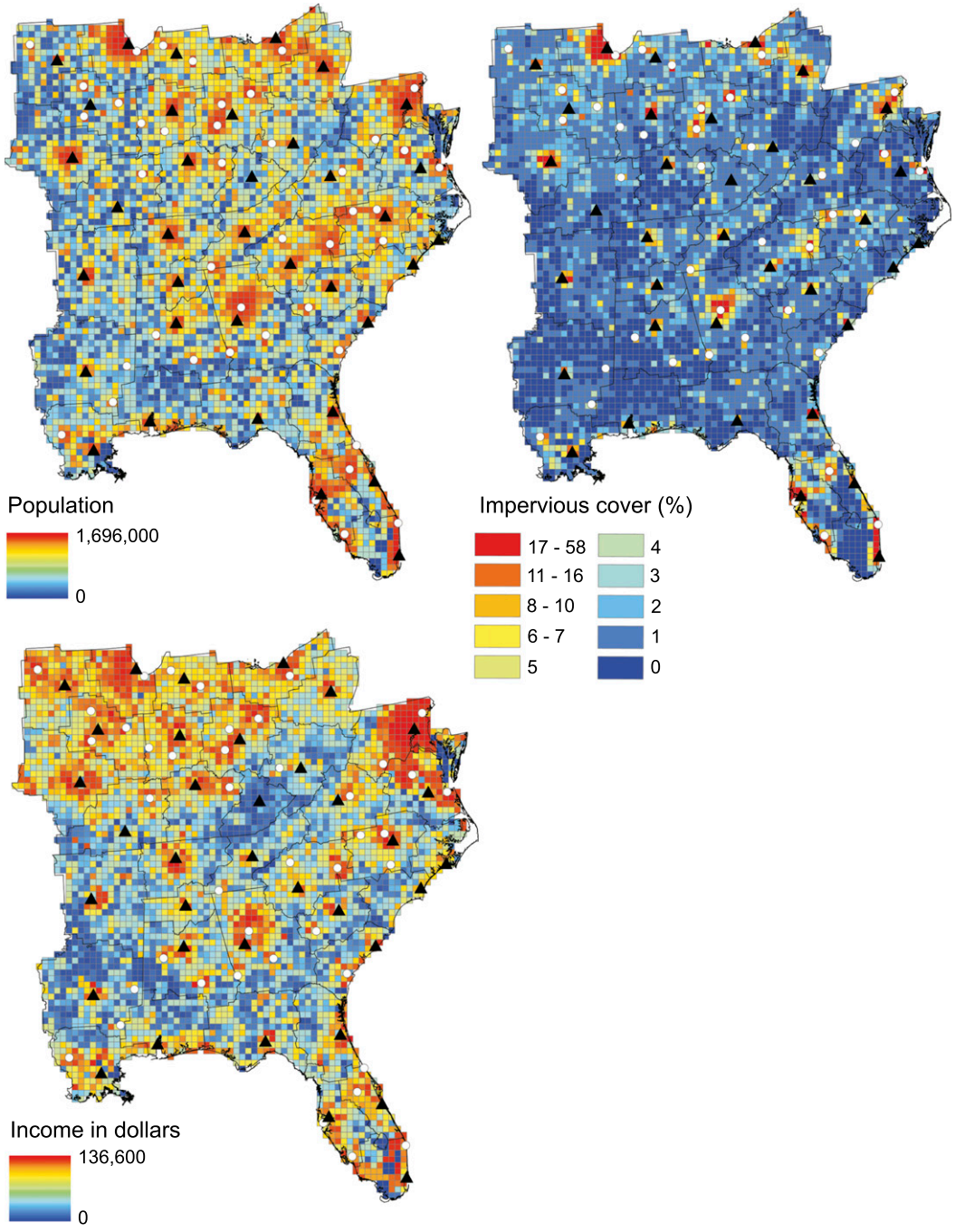

FIG. 2. Independent variables used in the analyses. Cell size is 20 km × 20 km.

Each grid cell contained the number of SVTs issued over the 8 years of the study, the percent impervious surface, total population, and median income. Grid cells over adjacent coastal waters of the study area were manually extracted from the dataset given that they did not record land surface properties. Buffering the data by selecting only grid cells at a uniform distance inland was considered. However, because there are several large coastal cities, manual deselection of grid cells was preferred.

c. *GWR*

GWR is a modeling technique that detects spatial nonstationarity in data relationships (Brundson et al. 1996). GWR accounts for the violation of independence that spatially distributed data manifest. By capturing the

stationary trend in the global relationship between a dependent and an independent variable, GWR can then estimate local regression parameters over actual geographic space and present the results as a map-based visualization. In local areas where the explanatory power of the independent variables exceeds or is less than that of the overall global trend, we can then begin to infer relationships about overwarning and underwarning and how it relates to CWA boundaries and patterns of population, income, and impervious surface.

We used a Poisson-based GWR model given that our dependent variable is warning counts per grid cell. In Eq. (1), y_i is the dependent variable at location i; N_i is the offset variable at the ith location; $\beta k(u_i, v_i)$ are coefficients that vary based on location; u_i and v_i are x and y coordinates of the ith location, respectively; and $x_{k,i}$ is the kth independent variable at location i,

$$y_i \sim \text{Poisson}\{N_i \exp[\Sigma_k \beta_k(u_i, v_i) x_{k,i}]\}. \quad (1)$$

GWR requires specification of two parameters. Bandwidth is the distance or area under which the relationship between the dependent and independent variable is spatially assessed. Bandwidth can have a large impact on GWR coefficients. As the bandwidth increases, the GWR coefficient estimates approach those of a global model, and the spatial pattern of the GWR coefficients will appear increasingly smooth across the study area. On the other hand, if a smaller bandwidth is used, then the GWR coefficient estimates depend on the observations in close proximity to the subject point and the coefficient estimates change rapidly over space (Fotheringham et al. 2002; Guo et al. 2008). The corrected Akaike information criterion (AICc) is a value representing divergence between observed and fitted values for a model. It was used to select bandwidth. The optimal bandwidth is the one that minimizes the AICc. Comparisons of the AICc values for the non-GWR and the GWR regressions can be used to gauge the contribution of spatial structure to the regressive relationship. The other specification required in GWR, the kernel, determines how observations are geographically weighted in the model. The type of kernel to use is based on the distances between observations. A fixed kernel is appropriate when the data are regularly positioned across the study area, with little to no clustering.

To perform Poisson GWR, we employed the software program GWR, version 4 (GWR4; Nakaya et al. 2009; Nakaya 2015; http://gwr.maynoothuniversity.ie/). Data for each grid cell were converted to a centroid. A fixed bisquare kernel was used in GWR4 to weight these equally spaced data. The bisquare distance decay function assigns zero weight to any value falling outside of the bandwidth and provides a much steeper curve for spatial weights than a Gaussian kernel. Bandwidth distances and their AICc values were calculated from an interval search for an optimal bandwidth bounded by 20 km (only the eight contiguous neighbors) as a minimum up to 200 km in intervals of 10 km.

Instead of a local variance explained (R2), Poisson models in GWR4 provide a global and a local percent deviance explained (Pdev). Term Pdev is a pseudo-R2 statistic that provides an indication of the goodness of fit in the model. The higher the Pdev, the better the model fit (Nakaya 2015). In the case of Pdev = 1, the model predictions are equal to the observed ones. Negative values are possible with the pseudo R2 calculated in GWR4, thus comparisons of Pdev from one independent variable to another are best approached as relative.

GWR also produces local regression coefficients that can track how an independent variable can shift in the direction of its association with the dependent variable across the study area beyond that of the global trend. Positive local coefficients indicate a disproportionate local increase in SVT counts relative to an increase in the independent variable. Negative coefficients indicate a lowering of SVT counts with an increase in the independent variable beyond that accounted for in the global model. Thus, the coefficient tells you how much the SVT counts are expected to increase (if the coefficient is positive) or decrease (if the coefficient is negative) when that independent variable increases. However, the complexity that allows GWR to elaborately illustrate local spatial relationships also engenders less certainty in the interpretation of coefficients when collinear independent variables are used in a single model (Wheeler and Tiefelsdorf 2005; Charlton and Fotheringham 2009). For that reason, we performed univariate regressions on our three independent variables.

Values for t can be used to quantify the statistical strength in the relationship between the independent and dependent variable. For Poisson GWR, t values are expressed as a pseudo t (estimate/standard error) in order to assess whether the spatial variation in a coefficient is significantly different from zero. The greater the magnitude of t (it can be either positive or negative), the greater the evidence against the null hypothesis that there is no significant relationship between independent and dependent variables. The closer t is to 0, the more likely there is no significant difference. Given that the t values are approximations, the usual 95% thresholds of ± 1.96 were used in a purely informal sense for evidence of parameter estimates that are significantly different from zero.

The spatial patterns of standardized residuals can be used to identify locations that deviate from the global regressive relationship. If standardized residuals are clustered, it can indicate that another factor or variable is shaping the distribution of the dependent variable.

Moran's *I*, a measure of spatial autocorrelation, was calculated for the standardized residuals of each independent variable to determine whether residuals were randomly distributed, clustered, or evenly dispersed. When the *Z* score or *p* value indicates statistical significance, a positive Moran's *I* index value indicates tendency toward clustering. A negative Moran's *I* index value indicates tendency toward dispersion.

3. Results

Total warning counts did not exhibit latitudinal trends, although they were somewhat expected given the north-to-south gradient in moisture and convective potential energy in our study area (Fig. 3). Instead, variability in warning counts was more associated with CWA boundaries and WFO city locations. These boundary and city effects were pronounced in North and South Carolina (Carolinas) and north into Virginia, Kentucky, and Tennessee, as well as parts of Mississippi and Louisiana. The highest total warnings per square kilometer were for grid cells in the CWAs of South Carolina.

Verified counts tended to increase around WFO cities in eastern CWAs (Fig. 3). By contrast, higher counts of unverified warnings were concentrated in the western half of our study area (Fig. 4). Unverified counts also tended to peak near WFO cities in some but not all CWAs. Verified warnings per square kilometer were highest for the CWAs in South Carolina.

Unverified warnings per square kilometer were highest in the CWA for Mobile, Alabama. Two of the largest metropolitan areas in our study—Chicago, Illinois, and Atlanta—had comparatively low counts for both verified and unverified SVTs. False alarm rates also corresponded with CWA boundaries and peaked in coastal Louisiana (Fig. 4). In the western and central portions of the study area, many of the CWAs demonstrated a trend where the FAR was higher in the periphery of the CWA and lower as the WFO city was approached. The visual result was a ring effect, as seen in the St. Louis area.

Non–geographically weighted regression models reported a very weak relationship between warnings and the independent variables, for both verified and unverified counts (Table 2). All of the six individual non-GWR models had low percent deviance explained. Coefficients were very close to zero. In contrast, global explained deviance for GWR models was high for all independent variables, ranging from 0.67 to 0.81 and accompanied by large reductions in AICc values compared to the non–geographically weighted models. Verified GWR global models explained slightly more deviance than unverified models. Optimal bandwidths among all six independent variables ranged from 50 to 80 km.

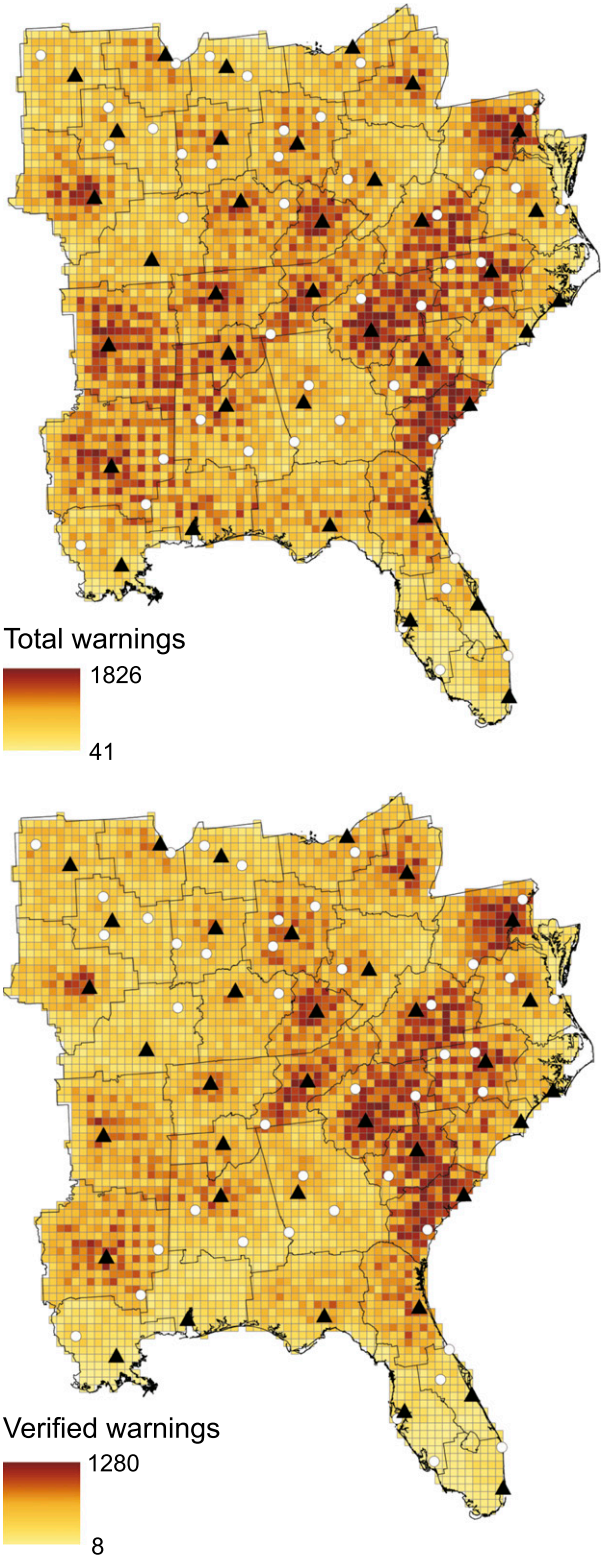

FIG. 3. Gridded (top) total severe thunderstorms warning counts and (bottom) verified warning counts only.

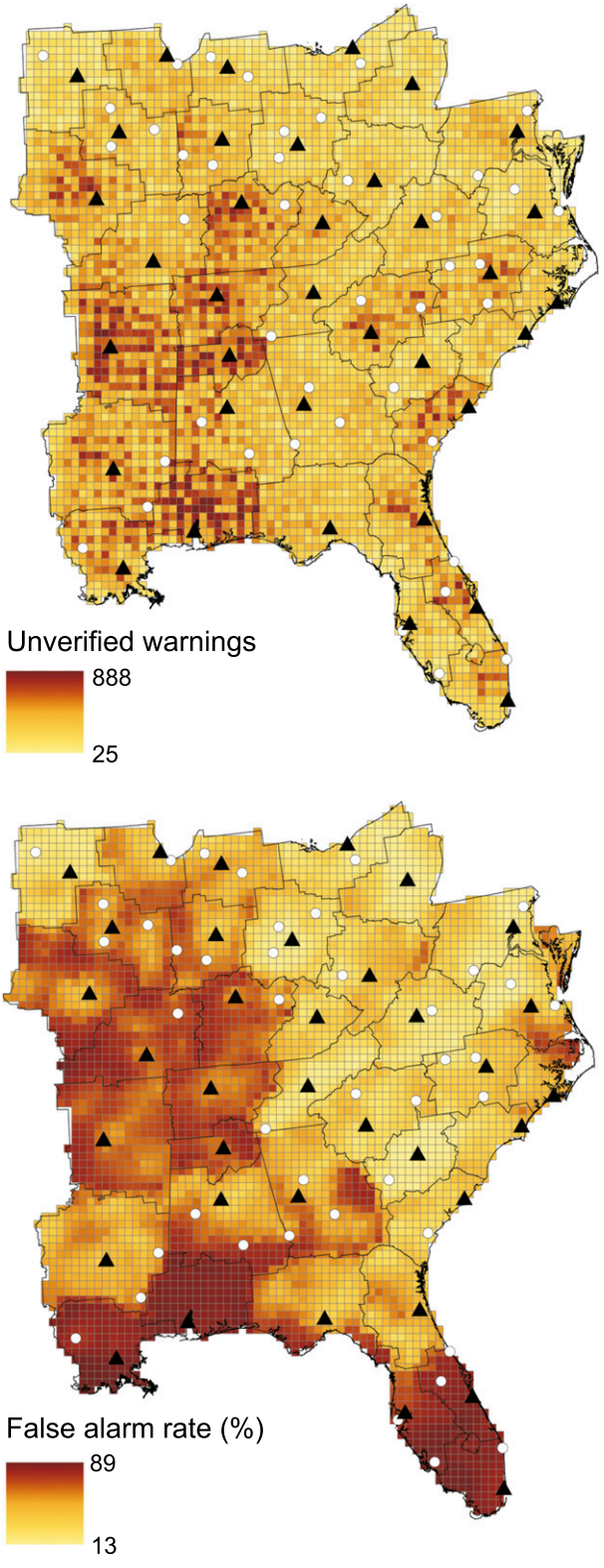

FIG. 4. Gridded (top) unverified warning counts and (bottom) false alarm rates.

Standardized global GWR coefficients suggested more variability in the spatial relationship between SVT counts and population than between SVT counts and the other two independent variables (Table 3). Standardized coefficients for population had a larger range, a higher mean and standard deviation, and a larger interquartile range for both unverified and verified warnings. Coefficient statistics were not as variable for impervious cover, and least of all for median income. However, these are measures of the central tendency of the global GWR coefficients. The spatial pattern of the local coefficients provides more detailed information.

a. Total population

Verified population coefficients were predominantly positive for many of the WFO locations (Fig. 5), implying that increases in population in these cities was associated with a disproportionately greater increase in verified warnings when compared to the global GWR model. These were supported by significant positive *t*-score values, as exemplified by St. Louis, Peachtree City–Atlanta area, and the Washington, D.C., corridor. Patterns of negative coefficients were seen in many rural areas, including eastern Kentucky, along the Gulf–Atlantic coastal plain, and in parts of Mississippi. With increases in population in these negative coefficient locations, warning counts tended to decrease disproportionately relative to the global trend. These negative coefficients were also associated with significant negative *t* scores. However, percent deviance was lower in the vicinity of WFO cities. Percent deviance tended to peak along the borders of each CWA as, for example, along the Ohio River in Kentucky and along the Georgia–South Carolina CWA boundaries.

Unverified counts (Fig. 6) had a similar distribution of positive and negative coefficients. Positive coefficients over WFO cities conveys that unverified warning counts tended to increase in the vicinity of more people but less so than verified counts. These areas of positive coefficients were also surrounded by more strongly negative coefficients when compared to the results for the verified counts. As based on *t* scores, the significance of unverified population coefficients was also weaker, particularly for positive values. Percent deviance had a similar range.

b. Percent imperviousness

GWR metrics for the relationship between percent impervious cover and verified warnings (Fig. 7) resembled those for population. Some WFO locations (St. Louis, Missouri; Jackson, Kentucky; and Indianapolis, Indiana) and some non-WFO cities (the Montgomery, Alabama–Columbus, South Carolina–Atlanta–Macon, Georgia, corridor; Asheville–Charlotte–Fayetteville area in North

TABLE 2. Non-GWR and GWR regression parameters.

	Verified warning counts			Unverified warning counts		
	Percent impervious	Total population	Median income	Percent impervious	Total population	Median income
Non-GWR Poisson regression						
Explained deviance (%)	0.87	0.87	1.52	0.69	0.31	0.35
Standardized coefficient	0.05	0.04	0.06	−0.04	−0.01	−0.03
AICc	460–592.3	460 593.8	457 568.1	220 896.7	221 739.8	221 633.3
GWR Poisson regression						
Explained deviance (%)	75	76	81	67	72	75
AICc	117953.3	110933	89718.9	73788.2	64737.9	59041.1
Bandwidth (m)	80 000	70 000	50 000	80 000	60 000	50 000
Standardized residuals						
Moran's *I*	0.05	0.01	−0.07	0.06	−0.01	−0.05
Z	4.2	1.2	−6.5	5.5	−0.9	−4.7
p	<0.001	0.22	<0.001	<0.001	0.36	<0.001

Carolina, and the Washington, D.C.–Virginia area) had higher positive coefficients than population. Rural areas again had lower, more negative coefficients. Significant *t* scores were distributed across urban and rural regions, with the coefficients becoming nonsignificant at the interface between them. Percent deviance remained lower in and near WFO cities and tended to increase toward CWA boundaries. GWR metrics for unverified warnings were also similar to population (Fig. 8), except positive coefficients were less strongly positive. The significance of positive *t* scores was also weaker and contracted around cities. A larger area of nonsignificant *t* scores developed in the transition zone between cities and more rural locations. Local percent deviance explained remained higher outside of cities.

c. *Median income*

Median income had finer-scale variability in the GWR metrics (Figs. 9 and 10) than population and impervious surface. This was also reflected in its optimal bandwidth, which was smaller than that of population and impervious cover. Magnitude and range of the standardized coefficients were relatively small compared to the other two independent variables. A few cities had weak positive coefficients for verified and unverified counts (Greenville, South Carolina; and Nashville and Knoxville, Tennessee). Weak negative relationships were less common but present for some WFOs (Huntsville, Alabama, and Jackson, Kentucky). Percent deviance was more heterogeneously distributed but still tended to peak outside of cities.

d. *Standardized residuals*

For total population, the residuals for verified and unverified counts were randomly distributed (Table 2). This implies that the GWR model performs equally well across the study area. However, residuals for impervious cover were clustered for both count types. Clustering of larger residuals for verified counts were centered around WFOs chiefly in the Carolinas.

Clustering of unverified residuals was visible in CWAs in the western and southern parts of the study area. These clusters reflect how individual CWA identity is important to the relationship between warning counts and impervious cover. Median income residuals for both count types were dispersed, suggesting that its GWR

TABLE 3. Descriptive statistics for local GWR coefficients.

	Percent impervious	Total population	Median income
	Verified counts		
Min–max	−2.2 to 4.1	−4.2 to 10.6	−1.2 to 1.6
Mean ± std dev	−0.01 ± 0.3	−0.07 ± 0.73	0.07 ± 0.22
Median	0.02	−0.02	0.07
Lower–upper quartile	−0.13 to 0.11	−0.25 to 0.16	−0.04 to 0.19
	Unverified counts		
Min–max	−2.5 to 2.2	−7.6 to 5.1	−1.8 to 1.3
Mean ± std dev	−0.13 ± 0.28	−0.36 ± 1.18	0.04 ± 0.21
Median	−0.07	−0.14	0.04
Lower–upper quartile	−0.24 to 0.02	−0.58 to 0.03	−0.08 to 0.16

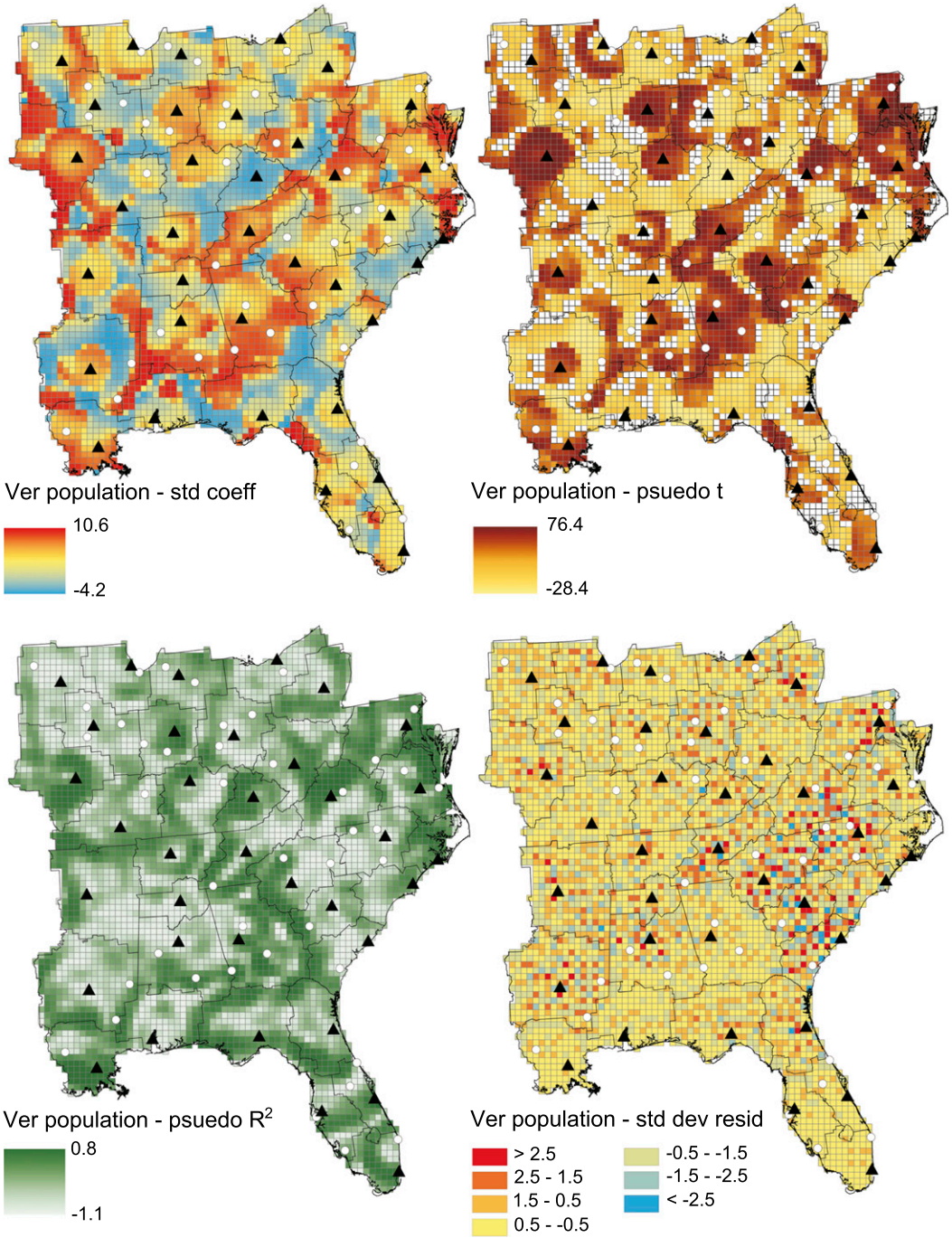

FIG. 5. GWR metrics for total population and verified warnings.

model tended to perform more evenly across the study area than expected.

4. Discussion

The overall pattern of total, verified, and unverified SVTs did not show a strong geographical gradient in severe thunderstorm frequency. Even though the thermodynamic environment for severe thunderstorm development is comparatively weaker in northern and coastal areas than in central and southern parts of the study region, changes in warning counts were more visually associated with CWA boundaries. Global GWR models confirmed that more than half of the

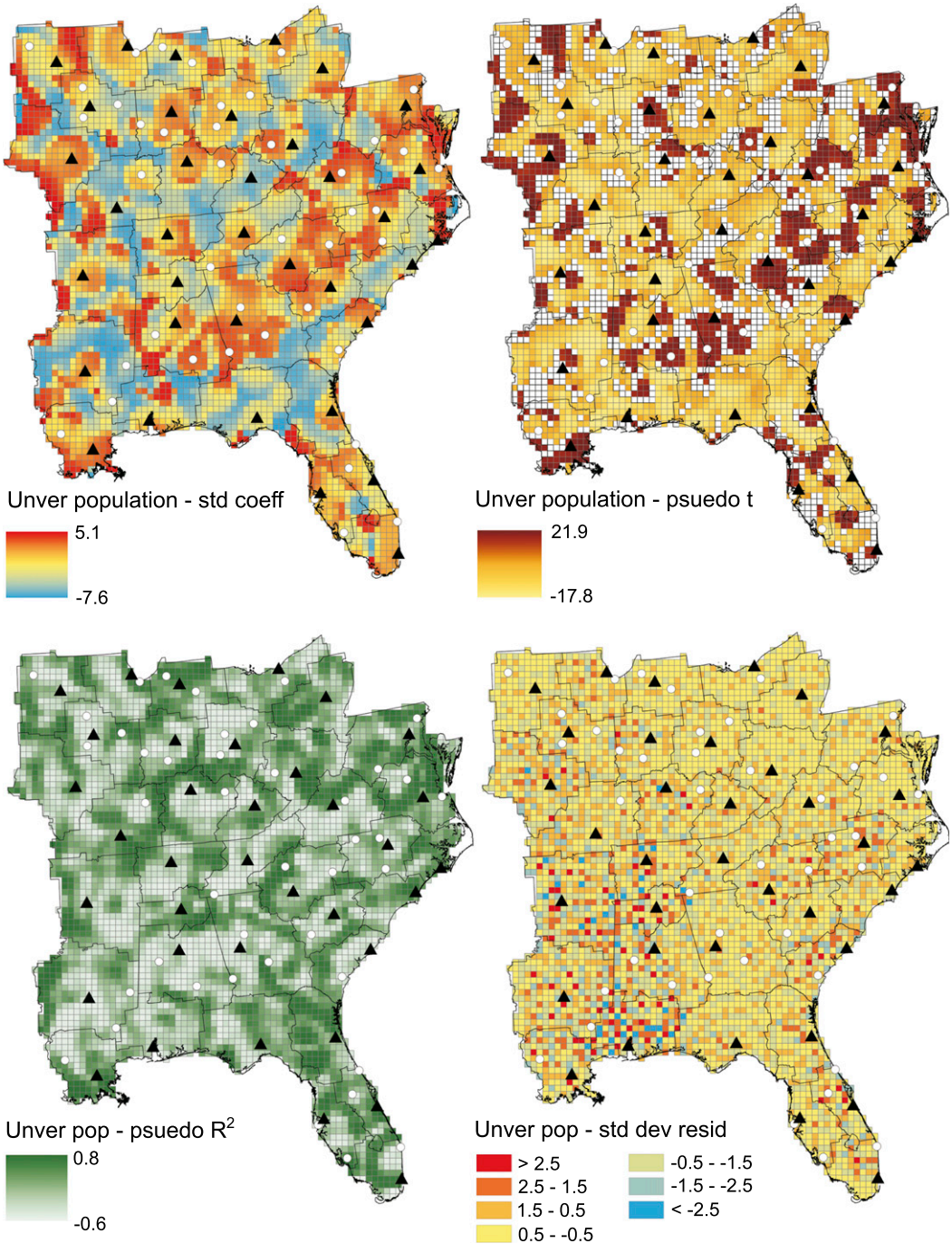

FIG. 6. GWR metrics for total population and unverified warnings.

variance (Pdev) in the distribution of SVTs could be attributed to the underlying spatial distribution of population, percent impervious, and median income. These findings suggest that human factors are strongly embedded in the historical spatial patterns of severe thunderstorm warning issuance and verification. Based on the descriptive statistics for the GWR standardized coefficients, warning counts are more sensitive to changes in population counts, followed by impervious cover, and then median income.

Verified warnings increased disproportionately as the population and impervious cover increased near cities. This could be expected, as more people equates to a greater likelihood of warning detection and postevent

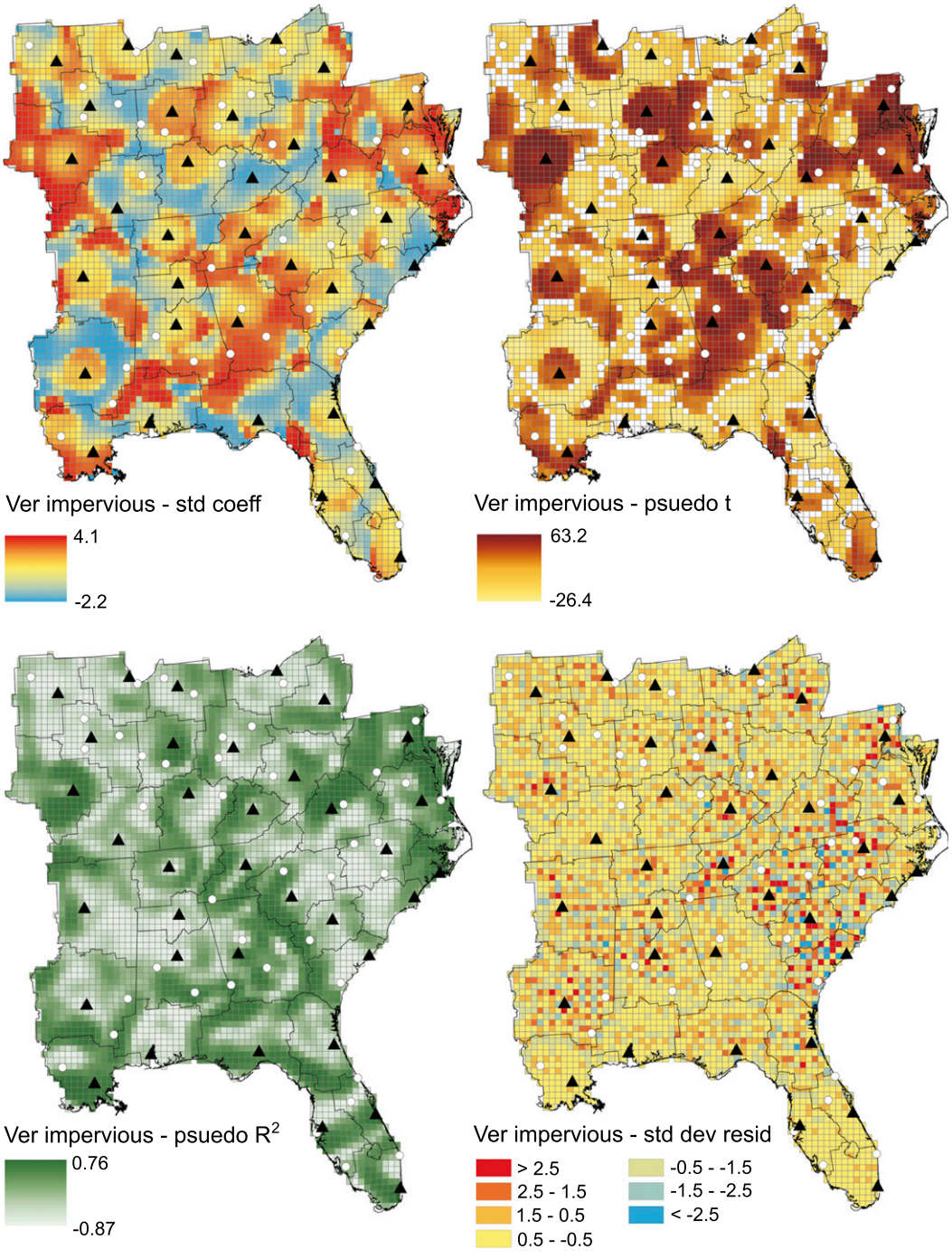

FIG. 7. GWR metrics for impervious cover and verified warnings.

verification. However, we found that there were also higher unverified counts around cities. For unverified warnings to show an enhanced local positive association with population and impervious cover in tandem with verified counts suggests a tendency for forecasters to err on the side of overissuance rather than underissuance around developed areas. Several cities stand out in this regard. Higher positive coefficients and significant positive t values for verified and unverified warnings were observed for the Washington, D.C.–Virginia–Maryland corridor, St. Louis, and for the chain of cities that extend northeast from Atlanta and into the Carolinas. The converse of this pattern was also present in less populated regions of the study area.

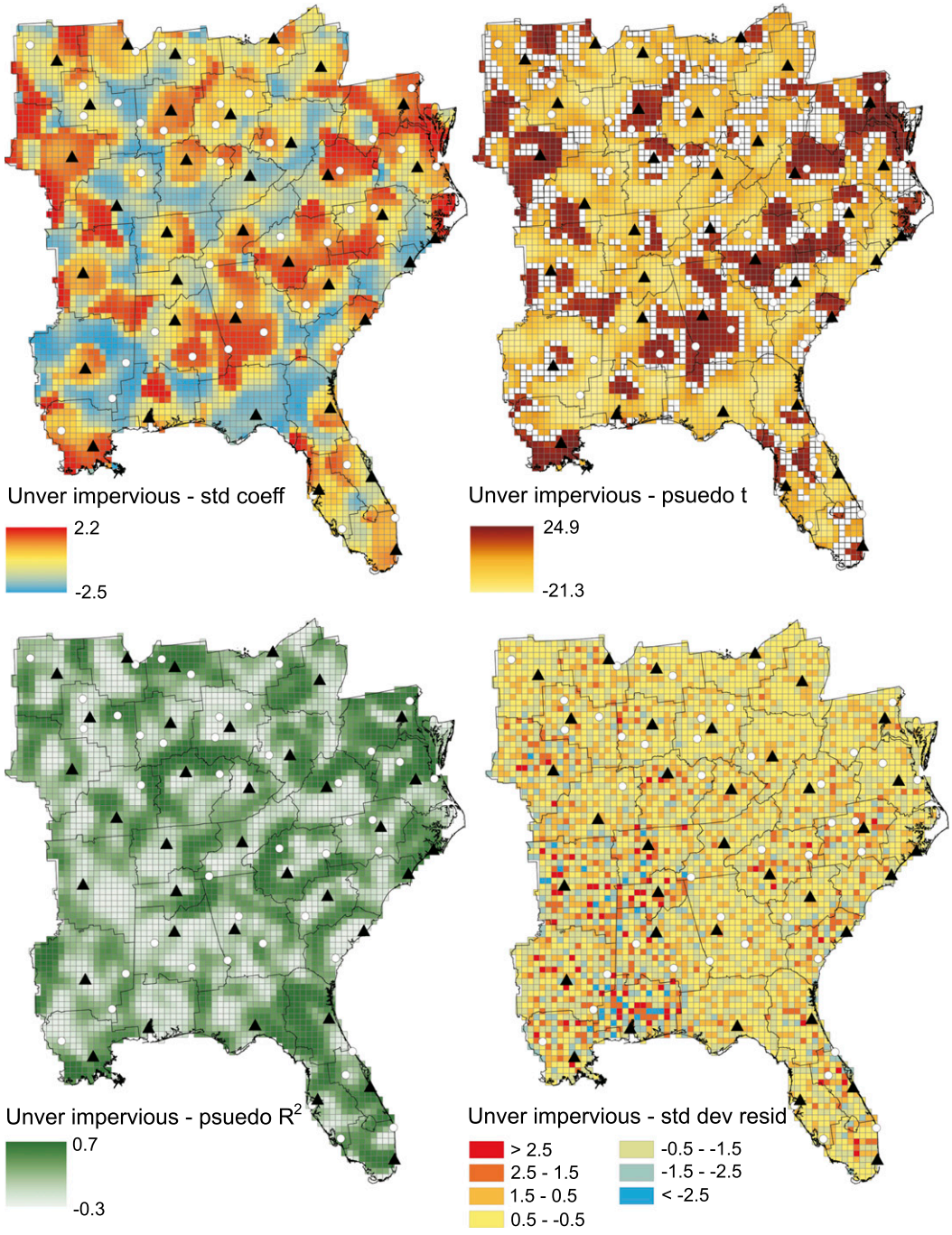

FIG. 8. GWR metrics for impervious cover and unverified warnings.

Near smaller cities, verified and unverified counts decreased disproportionately as populations increased. Jackson and Paducah, Kentucky, two of the smaller WFO cities, had negative coefficients for population and impervious surface. Overall, the pattern of coefficients for verified and unverified warning counts transitioned from positive to negative when moving from more urban and developed corridors to outlying rural areas and smaller towns.

Local percent deviance was lower in developed areas. However, this is not necessarily counterintuitive to the interpretation that populated areas are disproportionately favored over rural ones for the issuance of severe thunderstorm warnings. For one reason, the decision to

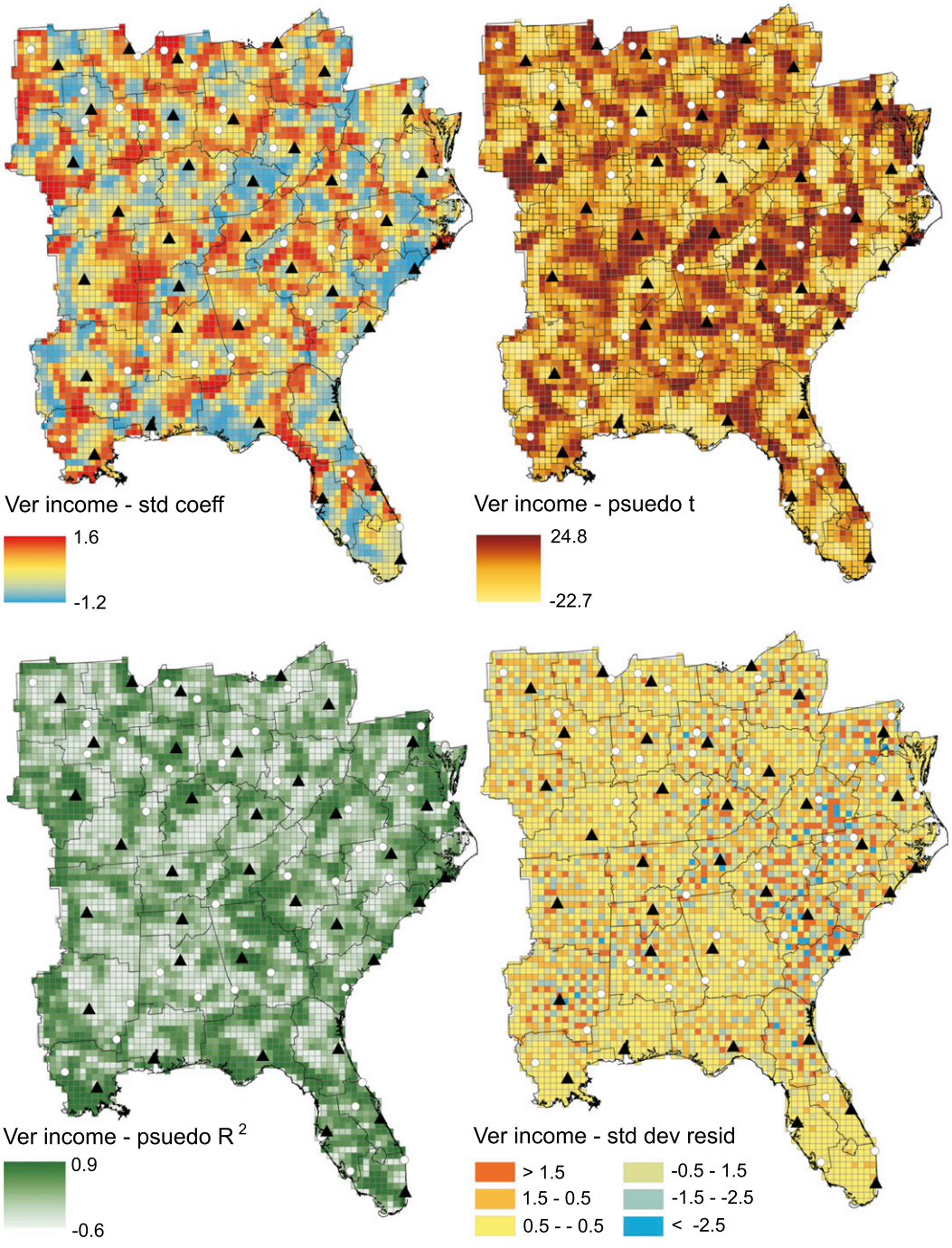

FIG. 9. GWR metrics for median income and verified warnings.

issue a warning near a city could involve a larger number of factors. Whether it is day or night, or rush hour, what season of the year it is, the history of past severe weather impacts, and the particulars of each city's infrastructure and land use patterns are all considerations that might come into play. Since this would imply greater degrees of freedom for the issuance of warnings around cities and developed corridors, more deviance could arise in the relationship of warning issuance to our independent variables. As observed, explained variance was actually higher in the rural, peripheral areas of CWAs, near their borders. Here, the decision process may involve a smaller number of variables to weigh when issuing a warning. The ring of higher percent deviance around

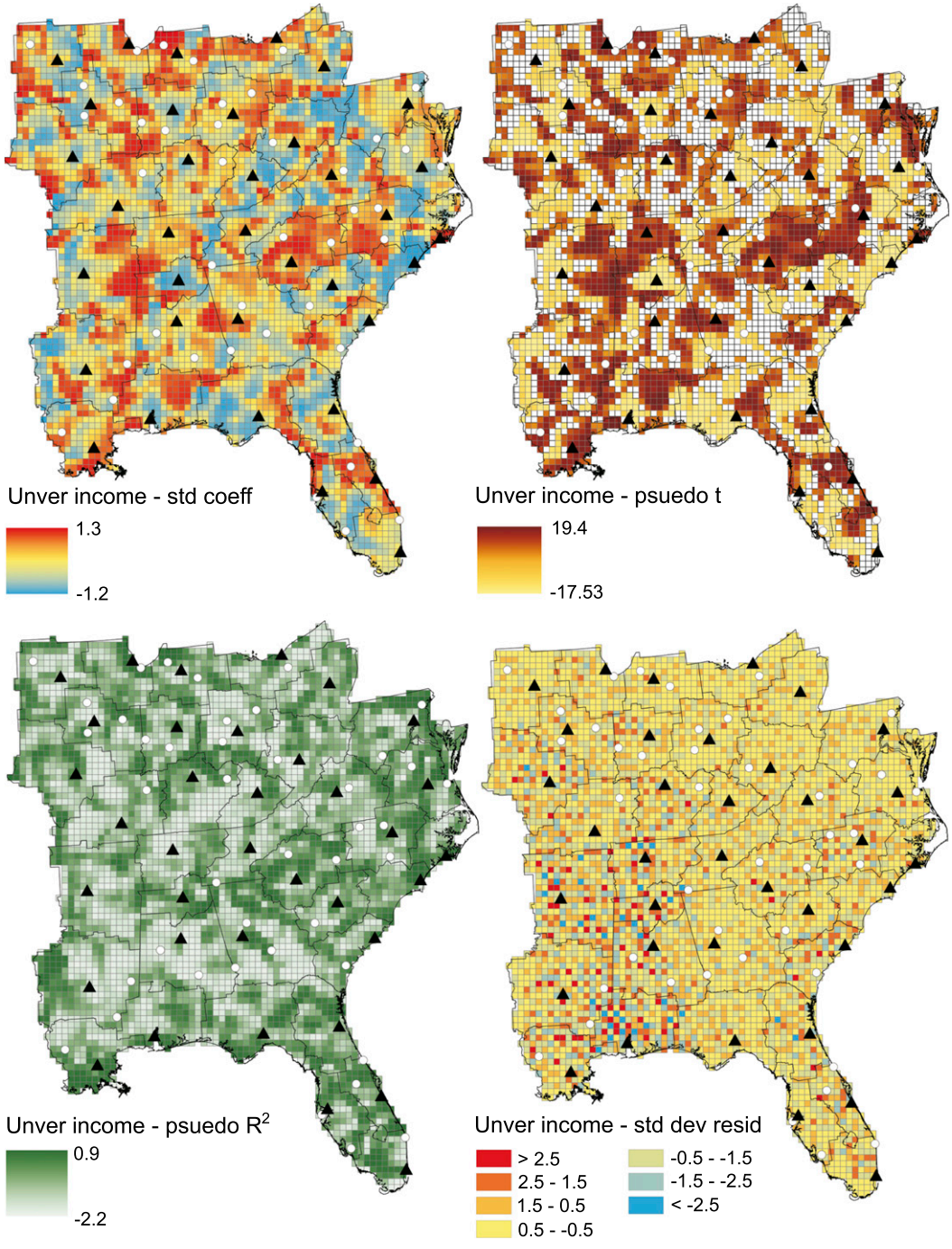

FIG. 10. GWR metrics for median income and unverified warnings.

a city or along CWA boundary can be interpreted as a consequence of these differences in decision strategies. New Orleans, Louisiana, Knoxville, and Nashville have better model performance just outside of the city center or along their forecast boundary, suggesting that at some point from the city center, warning issuance becomes a less contextual decision to make. However, some cities retained high percent explained variance for population and impervious cover closer to their centers, such as St. Louis and Indianapolis. Here, less deliberation may play into warning urban populations despite the larger number of human factors to consider.

Along with a predisposition to overwarn in populated areas, other factors offer alternative explanations. There

could be missed verifications by spotters and the general public, even though their density around WFOs and other cities would be higher. The cone of silence around Doppler radar could predispose a forecaster to issue warnings for borderline severe storms given that some aspects of imaging may not be optimal (Davis and LaDue 2004), although direct visual assessment of an impending nearby thunderstorm would seem likely. Issuing warnings at the county level and for individual storm polygons could also affect the distribution of both verified and unverified warning counts. Finer grain WFO-specific practices shaping warning issuance frequency and the relationship between cancelled county and continued storm-based polygon warnings may also contribute (Harrison and Karstens 2017). Differences in thunderstorm types (supercell, pulse, etc.) across the study area could also affect issuance, verification, and accuracy play a role (Guillot et al. 2008), for example, verified warning peak in states east of Atlanta and unverified warnings peak in states to the west. Speculatively, this may be related to the different kinds of thunderstorms more typical of these two regions on either side Georgia. The more western locations are more likely to experience supercell thunderstorms than the Atlantic coastal plain, and greater care may be taken to warn for them even in more sparsely populated areas.

Urban meteorological influences could also be expected to play a role in warning issuance and verification of severe thunderstorms. While impervious cover and total population are highly correlated ($r = 0.92$), impervious cover did not have the same GWR coefficient values. This suggests that impervious cover had a different regressive relationship with warning counts in comparison to population. Urban land cover and associated aerosol air pollution can modify thunderstorm convection (Saide et al. 2015; Dou et al. 2015; Yang et al. 2016). As land cover changes, thermodynamic properties of the atmosphere change. Aerosols link to storm severity through their modification of the vertical development of thunderstorms and how quickly raindrops coalesce and fall (Rosenfeld et al. 2008). Thunderstorms may also split in the vicinity of cities and then strengthen after merging downwind (Niyogi et al. 2011). These phenomena have been observed or modeled for Washington, D.C., and Baltimore, Maryland (Ntelekos et al. 2008; Zhang et al. 2011); the Indianapolis region (Niyogi et al. 2011); St. Louis (Rozoff et al. 2003); Atlanta (Stallins et al. 2006; Diem 2008; Haberlie et al. 2015); and Memphis (Ashley et al. 2012).

Speculatively, an unverified warning could have initiated as what appeared to be a severe storm, but subsequent exposure to humanized land covers and aerosol air pollution could alter these features and diminish its likelihood for verification. Still, there is substantial variation from city to city in the way thunderstorms are modified by these land cover and aerosol mechanisms (Ashley et al. 2012). Furthermore, aerosol effects on thunderstorms and their phenomena may extend over regional scales (Bell et al. 2009; Stallins et al. 2013), even well outside of cities. Locations with greater spatial and temporal variability in aerosol regimes and convective processes may also make the issuance of severe thunderstorm warnings challenging (Petersen and Rutledge 2001). The pattern of residuals for impervious cover (Table 2) was clustered, as might be expected if larger agglomerations of urban areas influence warning issuance and verification. Population, on the other hand, had randomly dispersed residuals, suggestive of a more global effect on the issuance of warnings, which could be derived from forecaster decisions about the demographic template more than any urban effect on thunderstorms.

Several WFO cities had noteworthy warning signatures in relation to their patterns of demographics and development. The Washington, D.C., area from Baltimore south to Norfolk, Virginia, coincides with high concentrations of wealth and a corridor of critical governmental infrastructure. The Asheville–Greenville–Charlotte corridor was another large, contiguous location with detectable human influences on warnings. St. Louis, Nashville, and Memphis also had statistically significant increases in verified and unverified warnings in relation to the global trend. The Atlanta–Macon–Columbus corridor and Jackson, Mississippi, stood out in comparison to their rural matrix. Chicago, despite its size, did not show any significant association of SVT counts with land cover or demographics. Many northern cities in this study had generally weaker positive and negative local departures from the global trend. This suggests that the latitudinal gradient in severe thunderstorm frequency, while not strongly apparent in the distribution of warnings, is still present.

5. Conclusions

More than half of the variance in the issuance of warnings across the entire study area may be related to population, percent impervious cover, and median income. WFOs, in addition to other medium to large cities, had increased numbers of both verified and unverified SVTs relative to the general trends across the study area. However, this variance is not simply a matter of more people equaling more warnings. The amount of local explained variance decreased in and near cities and increased toward CWA boundaries. One explanation for this may be related to the influence of context (i.e., time

of day, day of the week, season, and history of severe weather impacts) on informal aspects of the warning decision process in more developed locations. Along the periphery of forecast zones and in rural areas where explained variance was higher, contextual factors may carry less weight. There may be fewer impact scenarios to consider, resulting in higher explained variance in our models.

Because the purpose of severe thunderstorm warnings is to protect people and property, it could be argued that warning areas with more people and infrastructure is desired. A propensity to trigger more warnings in the vicinity of cities could be seen as a successful outcome and therefore relatively unproblematic. However, living in a place with fewer people should not be less safe than living in a place with more people. In smaller cities like Jackson and Paducah, Kentucky; and Peoria, Illinois; or Cedar Rapids, Iowa, our results indicate that, despite local increases in population, fewer warnings may be issued (relative to the global trend). Still, this study did not intend to take into account the way different kinds of thunderstorms impact SVT issuance. Isolated supercell and convective line storms are most likely to be accurately forecasted, as their higher radar intensities make them easier to identify than pulse and nonorganized storms. Information about preferential thunderstorm initiation zones, their tracks, urban influences, and the areas of their warning polygons would be useful for a more detailed interpretation of the findings of this study.

Given the strong CWA boundary and WFO location effects seen in the distribution of warnings, meteorological factors may not necessarily override social and cultural factors related to forecasting. This underscores the need for more behavioral research on forecasters' judgment and decision-making processes (Harrison and Karstens 2017). Our findings are echoed in the recommendations of Lindell and Brooks (2013), who stressed that there should be more study of forecasters' decision-making behaviors among NWS regions, WFOs, and between individual forecasters. The physical and informational structures of the NWS warning systems reflect a long history of research, planning, and financial investment. However, as the underling demographic template has changed, along with the technologies to monitor weather, it may be time to reconsider how the siting of weather offices and boundaries impact the warning process. Such boundary effects are known in geography as the modifiable areal unit problem (Dark and Bram 2007).

Ensuring equitable warning practices for all NWS subjects is a goal that may become more challenging over time. As forecast accuracy continues to increase, city-focused economies are likely to become more weather sensitive, and thus contribute to an increasing financialization of forecasting (Anbarci et al. 2011). Approaches to warning issuance may need to consider ways to balance the imperative to warn intensively capitalized and more densely populated regions with the need for equitability of warnings among individuals physically distant from these centers.

REFERENCES

Allen, J. T., M. K. Tippet, A. H. Sobel, and C. Lepore, 2016: Understanding the drivers of variability in severe convection: Bringing together the scientific and insurance communities. *Bull. Amer. Meteor. Soc.*, **97** (Suppl.), doi:10.1175/BAMS-D-16-0208.1.

Anbarci, N., E. Floehr, J. Lee, and J. J. Song, 2008: Economic bias of weather forecasting: A spatial modeling approach. Economic Series, Deakin University School of Accounting, Economics and Finance Working Papers SWP 2008/12, 42 pp.

——, J. Boyd III, E. Floehr, J. Lee, and J. J. Song, 2011: Population and income sensitivity of private and public weather forecasting. *Reg. Sci. Urban Econ.*, **41**, 124–133, doi:10.1016/j.regsciurbeco.2010.11.001.

Ashley, W. S., M. L. Bentley, and J. A. Stallins, 2012: Urban-induced thunderstorm modification in the Southeast United States. *Climatic Change*, **113**, 481–498, doi:10.1007/s10584-011-0324-1.

——, S. Strader, T. Rosencrants, and A. J. Krmenec, 2014: Spatiotemporal changes in tornado hazard exposure: The case of the expanding bull's-eye effect in Chicago, Illinois. *Wea. Climate Soc.*, **6**, 175–193, doi:10.1175/WCAS-D-13-00047.1.

Barnes, L. R., E. C. Gruntfest, M. H. Hayden, D. M. Schultz, and C. Benight, 2007: False alarms and close calls: A conceptual model of warning accuracy. *Wea. Forecasting*, **22**, 1140–1147, doi:10.1175/WAF1031.1.

Barrett, K. M., 2008: The county bias of severe thunderstorm warnings and severe thunderstorm weather reports for the central Texas region. M.A. thesis, Dept. of Geology, Baylor University, 126 pp. [Available online at http://hdl.handle.net/2104/5161.]

——, 2012: The spatial distribution of contiguous United States thunderstorm related short-fuse severe weather warnings. Ph.D. thesis, Texas State University, 248 pp. [Available online at https://digital.library.txstate.edu/handle/10877/4293.]

Bell, T. L., D. Rosenfeld, and K.-M. Kim, 2009: Weekly cycle of lightning: Evidence of storm invigoration by pollution. *Geophys. Res. Lett.*, **36**, L23805, doi:10.1029/2009GL040915.

Brooks, H. E., C. A. Doswell III, and M. P. Kay, 2003: Climatological estimates of local daily tornado probability for the United States. *Wea. Forecasting*, **18**, 626–640, doi:10.1175/1520-0434(2003)018<0626:CEOLDT>2.0.CO;2.

Brundson, C., A. S. Fotheringham, and M. E. Charlton, 1996: Geographically weighted regression: A method for exploring spatial nonstationarity. *Geogr. Anal.*, **28**, 281–298, doi:10.1111/j.1538-4632.1996.tb00936.x.

Charlton, M. E., and A. S. Fotheringham, 2009: Geographically weighted regression. White Paper, National Centre for Geocomputation, National University of Ireland Maynooth, 14 pp.

Dark, S. J., and D. Bram, 2007: The modifiable areal unit problem (MAUP) in physical geography. *Prog. Phys. Geogr.*, **31**, 471–479, doi:10.1177/0309133307083294.

Davis, S. M., and J. G. LaDue, 2004: Nonmeteorological factors in warning verification. *22nd Conf. on Severe Local Storms*, Hyannis, MA, Amer. Meteor. Soc., P2.7. [Available online at https://ams.confex.com/ams/11aram22sls/techprogram/paper_81766.htm.]

Diem, J. E., 2008: Detecting summer rainfall enhancement within metropolitan Atlanta, Georgia USA. *Int. J. Climatol.*, **28**, 129–133, doi:10.1002/joc.1560.

Dobur, J. C., 2005: A comparison of severe thunderstorm warning verification statistics and population density within the NWS Atlanta County Warning Area. *Fourth Annual Severe Storms Symp.*, Starkville, MS, East Mississippi Chapter National Weather Association and Amer. Meteor. Soc., D2–6. [Available online at https://www.weather.gov/media/ffc/SEconf.pdf.]

Doswell, C. A., III, H. E. Brooks, and M. P. Kay, 2005: Climatological estimates of daily nontornadic severe thunderstorm probability for the United States. *Wea. Forecasting*, **20**, 577–595, doi:10.1175/WAF866.1.

Dou, J., Y. Wang, R. Bornstein, and S. Miao, 2015: Observed spatial characteristics of Beijing urban climate impacts on summer thunderstorms. *J. Appl. Meteor. Climatol.*, **54**, 94–105, doi:10.1175/JAMC-D-13-0355.1.

Elsner, J. B., L. E. Michaels, K. N. Scheitlin, and I. J. Elsner, 2013: The decreasing population bias in tornado reports across the central plains. *Wea. Climate Soc.*, **5**, 221–232, doi:10.1175/WCAS-D-12-00040.1.

Fine, G. A., 2007: *Authors of the Storm: Meteorologists and the Culture of Prediction*. University of Chicago Press, 280 pp.

Fotheringham, A. S., C. Brundson, and M. Charlton, 2002: *Geographically Weighted Regression: The Analysis of Spatially Varying Relationships*. Wiley, 284 pp.

Frisbie, P., 2006: The population bias of severe weather reports west of the continental divide. *Natl. Wea. Dig.*, **30**, 11–16.

Fry, J., and Coauthors, 2011: Completion of the 2006 National Land Cover Database for the Coterminous United States. *Photogramm. Eng. Remote Sens.*, **77**, 858–864.

Gero, A. F., and A. J. Pitman, 2006: The impact of land cover change on a simulated storm event in the Sydney basin. *J. Appl. Meteor. Climatol.*, **45**, 283–300, doi:10.1175/JAM2337.1.

Guillot, E. M., T. M. Smith, V. Lakshmanan, K. L. Elmore, D. W. Burgess, and G. J. Stumpf, 2008: Tornado and severe thunderstorm warning forecast skill and its relationship to storm type. *24th Conf. on Interactive Information Processing Systems for Meteorology, Oceanography, and Hydrology*, New Orleans, LA, Amer. Meteor. Soc., 4A.3. [Available online at https://ams.confex.com/ams/88Annual/techprogram/paper_132605.htm.]

Guo, L., Z. Ma, and L. Zhang, 2008: Comparison of bandwidth selection in application of geographically weighted regression: A case study. *Can. J. For. Res.*, **38**, 2526–2534, doi:10.1139/X08-091.

Guyer, J. L., and M. L. Moritz, 2003: On issues of tornado damage assessment and F-scale assignment in agricultural areas. *Symp. on the F-Scale and Severe-Weather Damage Assessment*, Long Beach, CA, Amer. Meteor. Soc., 4.1. [Available online at https://ams.confex.com/ams/annual2003/techprogram/paper_57495.htm.]

Haberlie, A. M., W. S. Ashley, and T. J. Pingel, 2015: The effect of urbanization of the climatology of thunderstorm initiation. *Quart. J. Roy. Meteor. Soc.*, **141**, 663–675, doi:10.1002/qj.2499.

Hales, J. E. J., 1993: Biases in the severe thunderstorm data base: Ramifications and solutions. Preprints, *13th Conf. on Weather Analysis and Forecasting*, Vienna, VA, Amer. Meteor. Soc., 504–507.

Harrison, D. R., and C. D. Karstens, 2017: A climatology of operational storm-based warnings: A geospatial analysis. *Wea. Forecasting*, **32**, 47–6, doi:10.1175/WAF-D-15-0146.1.

Hoium, D. K., A. J. Riordan, J. Monaham, and K. K. Keeter, 1997: Severe thunderstorm and tornado warnings at Raleigh, North Carolina. *Bull. Amer. Meteor. Soc.*, **78**, 2559–2575, doi:10.1175/1520-0477(1997)078<2559:STATWA>2.0.CO;2.

IEM, 2016: Archived NWS watch/warnings. Iowa Environmental Mesonet, accessed 15 July 2016. [Available online at http://mesonet.agron.iastate.edu/request/gis/watchwarn.phtml.]

Lindell, M. K., and H. Brooks, 2013: Workshop on Weather Ready Nation: Science Imperatives for Severe Thunderstorm Research. *Bull. Amer. Meteor. Soc.*, **94** (Suppl.), doi:10.1175/BAMS-D-12-00238.1.

Morss, R. E., and F. M. Ralph, 2007: Use of information by National Weather Service forecasters and emergency managers during CALJET and PACJET-2001. *Wea. Forecasting*, **22**, 539–555, doi:10.1175/WAF1001.1.

Nakaya, T., 2015: Geographically weighted generalised linear modeling. C. Brunsdon and A. Singleton, Eds., *Geocomputation: A Practical Primer*, Sage Publications Ltd., 201–220.

——, A. S. Fotheringham, M. Charlton, and C. Brunsdon, 2009: Semiparametric geographically weighted generalised linear modelling in GWR4.0. *Proc. 10th Int. Conf. on GeoComputation*, Sydney, NSW, Australia, GeoComputation International Steering Group, 5 pp. [Available online at http://www.geocomputation.org/2009/PDF/Nakaya_et_al.pdf.]

Niyogi, D., P. Pyle, M. Lei, S. Pal Arya, C. M. Kishtawal, M. Shepherd, F. Chen, and B. Wolfe, 2011: Urban modification of thunderstorms: An observational storm climatology and model case study for the Indianapolis urban region. *J. Appl. Meteor. Climatol.*, **50**, 1129–1144, doi:10.1175/2010JAMC1836.1.

NOAA, 2016: U.S. climate regions. [Available online at https://www.ncdc.noaa.gov/monitoring-references/maps/us-climate-regions.php.]

Ntelekos, A. A., J. A. Smith, M. L. Baeck, W. F. Krajewski, A. J. Miller, and R. Goska, 2008: Extreme hydrometeorological events and the urban environment: Dissecting the 7 July 2004 thunderstorm over the Baltimore, MD Metropolitan Region. *Water Resour. Res.*, **44**, W08446, doi:10.1029/2007WR006346.

Paulikas, M. J., 2013: Examining population bias relative to severe thunderstorm hazard reporting trends in the Atlanta, GA metropolitan region. *Meteor. Appl.*, **21**, 494–503, doi:10.1002/met.1394.

Pennell, A., 2009: The influence of tornadic experiences on severe weather preparedness: A comparative study of Abilene, Texas and Huntsville, Alabama. *Natl. Wea. Dig.*, **33** (1), 103–118.

Petersen, W. A., and S. A. Rutledge, 2001: Regional variability in tropical convection: Observations from TRMM. *J. Climate*, **14**, 3566–3586, doi:10.1175/1520-0442(2001)014<3566:RVITCO>2.0.CO;2.

Ray, P. S., P. Bieringer, X. Niu, and B. Whissel, 2003: An improved estimate of tornado occurrence in the central plains of the United States. *Mon. Wea. Rev.*, **131**, 1026–1031, doi:10.1175/1520-0493(2003)131<1026:AIEOTO>2.0.CO;2.

Rosencrants, T. D., and W. S. Ashley, 2015: Spatiotemporal analysis of tornado exposure in five US metropolitan areas. *Nat. Hazards*, **78**, 121–140, doi:10.1007/s11069-015-1704-z.

Rosenfeld, D., U. Lohmann, G. B. Raga, C. D. O'Dowd, M. Kumala, S. Fuzzi, A. Reissell, and M. O. Andreae, 2008: Flood or drought: How do aerosols affect precipitation? *Science*, **321**, 1309–1313, doi:10.1126/science.1160606.

Rozoff, C. M., W. R. Cotton, and J. O. Adegoke, 2003: Simulation of St. Louis, Missouri, land use impacts on thunderstorms. *J. Appl. Meteor.*, **42**, 716–738, doi:10.1175/1520-0450(2003)042<0716:SOSLML>2.0.CO;2.

Saide, P. E., and Coauthors, 2015: Central American biomass burning smoke can increase tornado severity in the U.S. *Geophys. Res. Lett.*, **42**, 956–965, doi:10.1002/2014GL062826.

Sander, J. F., E. Faust, and M. Steuer, 2013: Rising variability in thunderstorm-related U.S. losses as a reflection of changes in large-scale thunderstorm forcing. *Wea. Climate Soc.*, **5**, 317–331, doi:10.1175/WCAS-D-12-00023.1.

Schmidlin, T. W., B. O. Hammer, Y. Ono, and P. S. King, 2009: Tornado shelter-seeking behavior and tornado shelter options among mobile home residents in the United States. *Nat. Hazards*, **48**, 191–201, doi:10.1007/s11069-008-9257-z.

Stallins, J. A., M. L. Bentley, and L. S. Rose, 2006: Cloud-to-ground flash patterns for Atlanta, Georgia (USA) from 1992 to 2003. *Climate Res.*, **30**, 99–112, doi:10.3354/cr030099.

——, J. Carpenter, M. L. Bentley, W. S. Ashley, and J. A. Mulholland, 2013: Weekend–weekday aerosols and geographic variability in cloud-to-ground lightning for the urban region of Atlanta, Georgia, USA. *Reg. Environ. Change*, **13**, 137–151, doi:10.1007/s10113-012-0327-0.

Sutter, D., and S. Erikson, 2010: The time cost of tornado warnings and the savings with storm-based warnings. *Wea. Climate Soc.*, **2**, 103–112, doi:10.1175/2009WCAS1011.1.

U.S. Census Bureau, 2013: American Community Survey. Subset used: 2007–2011, accessed 15 July 2016. [Available online at http://factfinder2.census.gov/faces/nav/jsf/pages/searchresults.xhtml?refresh=t.]

Wheeler, D., and M. Tiefelsdorf, 2005: Multicollinearity and correlation among local regression coefficients in geographically weighted regression. *J. Geogr. Syst.*, **7**, 161–187, doi:10.1007/s10109-005-0155-6.

Yang, X., Z. Li, L. Liu, L. Zhou, M. Cribb, and F. Zhang, 2016: Distinct weekly cycles of thunderstorms and a potential connection with aerosol type in China. *Geophys. Res. Lett.*, **43**, 8760–8768, doi:10.1002/2016GL070375.

Zhang, D.-L., Y.-X. Shou, R. R. Dickerson, and F. Chen, 2011: Impact of upstream urbanization on the urban heat island effects along the Washington–Baltimore corridor. *J. Appl. Meteor. Climatol.*, **50**, 2012–2029, doi:10.1175/JAMC-D-10-05008.1.